

High harmonic generation and ionization effects in cluster targets

M. Aladi, I. Márton, P. Rácz, P. Dombi, and I.B. Földes

Wigner Research Centre for Physics of the Hungarian Academy of Sciences, Association EURATOM HAS,
H-1121 Budapest, Konkoly-Thege u. 29-33, Hungary

(Received 19 March 2014; revised 4 July 2014; accepted 4 August 2014)

Abstract

High harmonic generation in gas jets was investigated in different gases up to more than 14 bar backing pressure. The observation of increase of harmonic intensity with increasing pressure and laser intensity shows evidence of the presence of clusters in Xe with an increased efficiency compared with He, whereas Ar is an intermediate case for which clusters will start to dominate above a certain backing pressure. Spectral investigations give evidence for tunable harmonic generation in a broad spectral range. A spectral shift of opposite signature caused by the free electrons in the focal volume and the nanoplasmas inside the cluster was observed.

Keywords: clusters; high harmonic generation; nanoplasmas; ultrashort pulses

1. Introduction

The most flexible tool for generating coherent extreme ultraviolet (EUV) radiation by an intense laser pulse is the generation of its high harmonics. The harmonics of ultrashort laser pulses in gases cover practically the full spectral range from the visible to kilo-electronvolt x-ray. In the interaction of an intense laser pulse with a gas consisting of atoms, molecules or – in the present case – clusters, optical ionization may occur as a result of the distortion of the Coulomb potential by the intense electric field^[1, 2]. The freed electron is driven by the laser electric field, and may recombine with its parent ion, emitting the excess energy in the form of a high energy photon. As this process is repeated every half-cycle, the temporal periodicity of the process leads to the appearance of discrete spectral lines at harmonics of the laser frequency. This half-cycle periodicity is the reason why in most cases odd harmonics are generated in gases up to a limit defined by the laser intensity and the ionization potential of the gas, giving an upper limit for the generated photon energies. A great deal of effort has been expended towards increase of the conversion efficiency of harmonics for better usability. High harmonic generation (HHG) from clusters seems to be a possible candidate for an efficient light source giving higher emission frequencies and higher conversion efficiency^[3, 4].

Although the higher conversion efficiency and higher observable harmonics are advantageous, the investigation

of HHG from clusters is not strongly prevalent because of two main reasons. The first reason is that although the conversion can be higher than in atomic gases, the ionization of clusters sets an upper limit for the obtainable intensity, similarly to that of atoms. Therefore, most of the recent efforts aim to use loose focusing^[5–7] and consequently a long homogeneous target material for harmonic generation. Clearly, it is not easy to realize an elongated cluster source. The other obstacle for a broader application is that the mechanism of HHG from clusters is still a subject of intense debate^[8]. Apart from the traditional three-step model which is based on the recombination to the same atom, models have been developed in which recombination is considered to the neighbouring atoms^[9, 10], which may even produce incoherent radiation as there will be no phase locking between the two atomic wavefunctions^[11]. Ruf *et al.*^[8] suggests an alternative with tunnel ionization from a partly delocalized electron wavefunction and recombination to this wavefunction, i.e., to the cluster itself. In experiments the difficulty of separation of harmonics from the monomer atoms and from clusters makes it difficult to determine the actual mechanism of harmonic generation.

In the present work we aim to progress towards the ionization limit, i.e., we are investigating the limit where the ionization sets in with the signature of free electrons in the free space and inside the cluster as well. HHG is investigated in different gases, namely in He which is purely atomic, in Xe which generally forms clusters, and in transitory Ar where significant cluster generation sets in

Correspondence to: I. B. Földes, Wigner Research Centre for Physics, H-1525 Budapest, POB 49, Hungary. Email: foldes.istvan@wigner.mta.hu

above a certain backing pressure of the pulsed valve source. Investigation of the pressure dependence of the harmonic intensity shows the effects of cluster generation. Detailed analysis of the harmonic spectra shows the tunability of the harmonic wavelength by the appearance of free electrons in the interaction range, and also the effect of free electrons inside the clusters.

2. Experimental

Harmonics were generated in gas jet targets using commercial valves of Parker Hannifin, Series 9. The original conical nozzle had an orifice of 1 mm diameter. In order to improve the gas jet target parameters, an additional nozzle with a cylindrical orifice of 0.7 mm diameter was used. The total gas density was measured using an x-ray shadowgraphic method for Ar and Xe, and thus the average density as well as the density distribution was determined in our earlier investigations^[12] from 2–12 bar backing pressure. In the case of a typical 1 ms opening time of our experimental series the density at ~ 1 mm from the nozzle tip was found to be as high as 10^{19} atoms cm^{-3} – depending slowly on the pressure – for both gases. Therefore, it seems to be reasonable to assume a similar density for He, as well.

The formation of clusters can be approximated by the semiempirical Hagena scaling parameter^[13], $\Gamma^* = k((d/\tan\alpha)^{0.85}/T_0^{2.29})p_0$, in which d is the diameter of the orifice in μm , p_0 is the backing pressure in mbar, T_0 is the temperature in Kelvin, and k is the condensation parameter^[13], which is equal to $k = 5500$ for Xe, $k = 1650$ for Ar and $k \approx 4$ for He. We approximate the jet expansion half-angle by $\alpha \approx 45^\circ$. Using this scaling parameter the average cluster size can be estimated^[13] as $\bar{N} = 33(\Gamma^*/1000)^{2.35}$, which can be plotted in our range of interest, i.e., 1–20 bar backing pressure at room temperature, for the gases used in Figure 1. Our earlier experimental investigations^[12] with the additional nozzle showed (Figure 3 therein) that the jet expansion half-angle was really $\alpha \approx 45^\circ$ without the additional nozzle, and even smaller, $\alpha \approx 30^\circ$, with the additional nozzle, giving even higher cluster sizes.

It can be seen that for He no clusters can be expected. The cluster sizes for Xe are significantly larger than for Ar, but with increasing pressure the size of the clusters is well above 1000 atoms even for Ar. These curves are estimated from the scaling law above^[13], which will be used throughout the remainder of the paper. The dotted horizontal line gives the limit above which the cluster effect seems to play a significant role in our observations. As we shall see below, its intersection with the Xe and Ar data is in agreement with the harmonic results which suggest the effect of clusters above 6 bar backing pressure in Ar and even for the lowest Xe backing pressures.

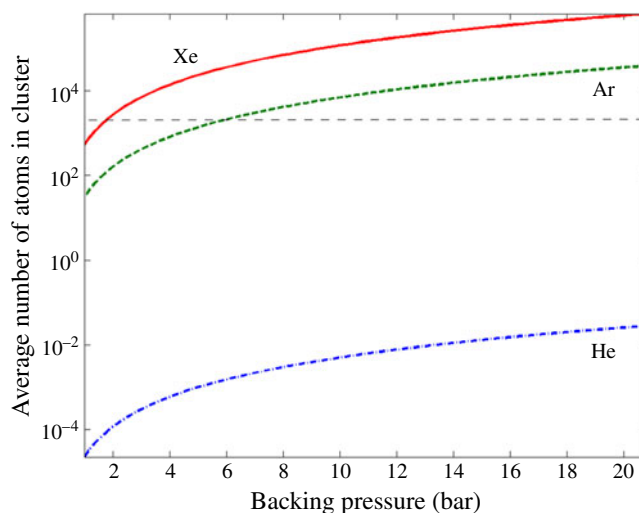


Figure 1. Pressure dependence of the average cluster size for He (dashed-dotted line), Ar (dashed line) and Xe (solid line) according to the Hagena scaling.

A Ti:sapphire laser beam was used in the experiments with 800 nm central wavelength and 1 kHz repetition rate. The pulse duration was 40 fs with 4 mJ pulse energy. The ~ 1 cm diameter beam was focused into the vacuum chamber by an $f = 30$ cm lens. The position of the valve could be varied relative to the focal plane by moving the lens parallel to the beam. A toroidal holographic grating (Jobin-Yvon) of 550 lines mm^{-1} collected the emitted high harmonic in the vacuum ultraviolet (VUV). Due to the loose focusing there was a danger that in this imaging spectrometer in which the valve–grating distance was only ~ 32 cm the grating might be damaged. Therefore the arrangement of Peatross *et al.*^[14] was used, which is a combination of a beam block at the centre of the incident beam and an aperture before the grating which suppresses the fundamental beam. The detector was a microchannel plate (MCP) with a phosphor screen. The visible light of the screen was imaged onto a CCD detector. This single-shot spectrometer provided a spectrum between 20 and 50 nm with a resolution of ~ 0.5 nm.

In the experiments, the intensity and spectral dependence of high harmonics were investigated for different gases in dependence on the pressure. For a comparison we chose the 30–50 nm wavelength range; thus, high enough harmonics could be observed with a single shot without moving the grating but in a range in which the reflectivity of the grating was still acceptable (note that it starts to decrease below 35 nm).

3. Results

HHG was observed in each gas from 1 to 20 bar backing pressure. Figure 2 illustrates the spectrum obtained from Ar at 14 bar backing pressure for a laser intensity of

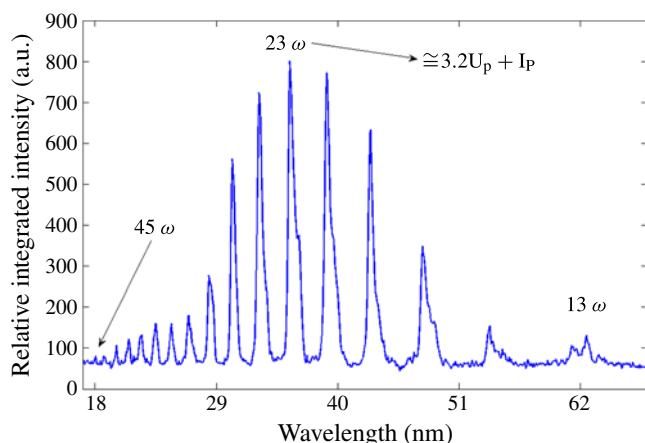


Figure 2. The HHG spectrum from Ar at 14 bar backing pressure and $10^{14} \text{ W cm}^{-2}$ intensity.

$10^{14} \text{ W cm}^{-2}$, in which case harmonics up to the 45th order were observed, which is nearly a factor of 2 higher than the ponderomotive cutoff limit at $I = 3.2U_p + I_p$, in which I_p is the ionization potential and U_p is the ponderomotive energy. Clearly, the intensity of the harmonics starts to drop at this limit. We can mention here that according to the documentation of the grating as obtained from Francelab its efficiency drops below 30 nm wavelength; therefore, the real intensity of the high harmonic orders is relatively higher than in Figure 2.

In order to compare the intensity dependence of HHG for different gases we chose a given harmonic order. Although the dependences are similar for different harmonic orders, the selection of a given pressure and harmonic order reduces the uncertainties, and it is thus illustrative for showing the qualitative behaviour. Figure 3 compares the intensity of a given harmonic order (15th in this case) for different gases, and here we can see that the conversion efficiency is highest for Xe, and it is significantly lower in the other two gases. In each case, after an initial increase of conversion efficiency with increasing intensity, it turns to saturation and then to a decrease of conversion efficiency above $1\text{--}2 \times 10^{14} \text{ W cm}^{-2}$. While the highest observed conversion efficiency in Xe cannot be fully attributed to the presence of clusters (even the atomic conversion efficiency of xenon is the highest one) the earlier saturation refers to the lower ionization potential.

The existence of clusters can be confirmed when investigating the pressure dependence of HHG, especially for Ar where the change is abrupt. Figure 4 compares the efficiency of the 25th harmonic for the three gases as a function of backing pressure. At low argon pressures and for He the increase of intensity with pressure is slow, even less than linear. In the case of argon a steep increase of efficiency starts above 6 bar backing pressure. This steeper increase can be attributed to the effect of clusters that appear with increasing pressure. Although the range of steeper increase is not sufficient for fitting, the steeper increase is

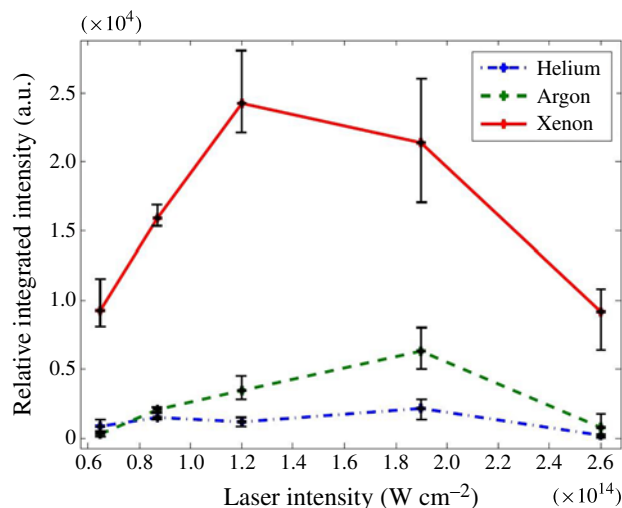


Figure 3. Intensity dependence of the 15th harmonic for different gases at 6 bar backing pressure.

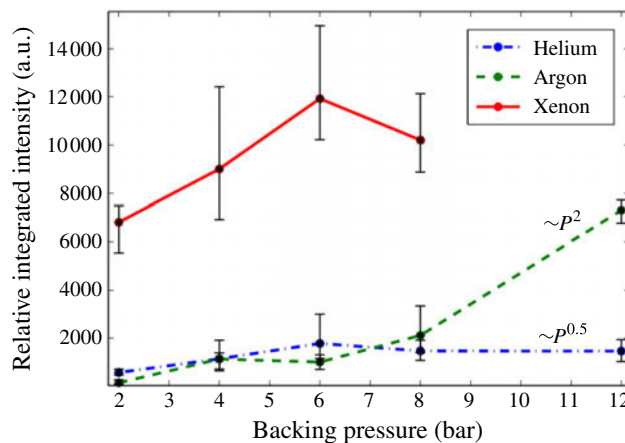


Figure 4. Comparison of the pressure dependence of the 25th harmonic at $6.5 \times 10^{13} \text{ W cm}^{-2}$ intensity in He, Ar, and Xe.

approximately quadratically dependent on the pressure. This steeper dependence is expected for clusters^[3], especially above 6 bar in Ar where the size of the clusters starts to become significant, i.e., more than 1000 atoms. It should be noted that this cluster size is the same as for Xe already at 1 bar; therefore, we can assume that for Xe cluster effects dominate for the whole pressure range of our investigations. In Xe the pressure dependence starts steeply – similarly to Ar above 6 bar – then it shows a saturation, probably because of propagation effects in the high density material.

It should be noted that our observations differ slightly from those of Donnelly *et al.*^[3], as they claimed an even stronger, cubic pressure dependence in the case of cluster targets. This difference can be partly caused by the different pulse duration of the laser, which was significantly longer in their work, 150 fs as compared with our 40 fs duration. Another possibility is that due to the different shapes of the valves

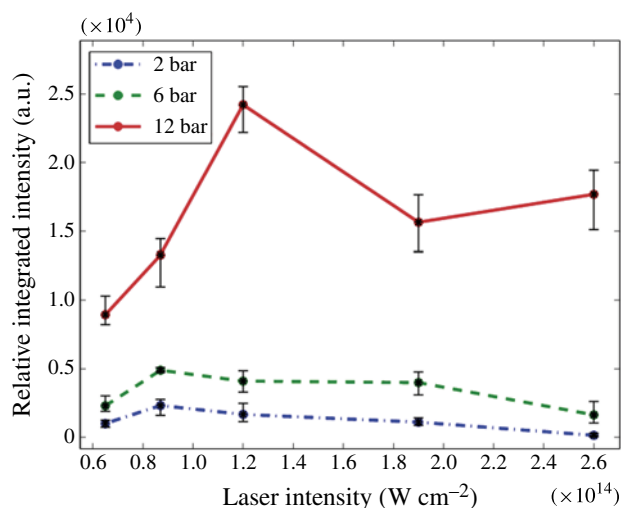


Figure 5. Intensity dependence of 25ω generation for Ar at 2, 6 and 12 bar backing pressure.

the densities were different in the different experiments^[12]. Last but not least, propagation effects may play an important role in the not too steep pressure dependence in our case, as this explanation is supported by the observation of intensity saturation in Xe for high pressure, as illustrated in Figure 4.

The observation that argon seems to display a sharply increased conversion efficiency with the appearance of clusters shows that we can investigate the intensity dependence of harmonic conversion for different backing pressures when clusters are generated, i.e., above 6 bar, and when not. Figure 5 illustrates the intensity dependence for 2 bar backing pressure where cluster formation is negligible, for 12 bar

with strong clusterization, and for 6 bar which is intermediate. Clearly, harmonic conversion is significantly higher for the largest clusters (12 bar), and at the lowest intensities, the conversion efficiency increase is steeper than for the cases with lower pressures and modest cluster formation. On the other hand, the saturation due to ionization of the gas is similar for clusters to that for atomic gases. Therefore, we can see that although clusters may really increase the conversion efficiency of harmonics, the ionization limit is not changed significantly.

Special emphasis was directed towards detailed spectral analysis of the harmonics. Here, the results were collected for the case in which the gas jet was behind the focus of the laser, i.e., in the diverging beam; thus, throughout the experiments the short trajectories of electrons in the HHG process were probably dominant^[15]. As was expected, the spectral width of the harmonics was significantly broader in Xe, where the beam interacted with clusters, than in He, in which no clusters were present. While the typical spectral width of harmonics in the wavelength range of 30–50 nm did not show significant pressure dependence and its full width varied between 1.4 and 2 nm, the spectral width of the harmonics for Xe showed a near linear increase with increasing pressure. As an example, in the case of the 15ω radiation the spectral width was 1.9 nm for 2 bar backing pressure, and it reached 4.5 nm width in the case of 12 bar. These observations agree with earlier results, e.g., with fullerene targets^[16].

It was discovered in the 1990s that in the case of moving the gas target relative to the focal plane a spectral blue shift can be observed due to the varying free electron density, thus providing even a tunability of high harmonics^[17]. Figure 6 clearly shows this effect, namely that a significant blue

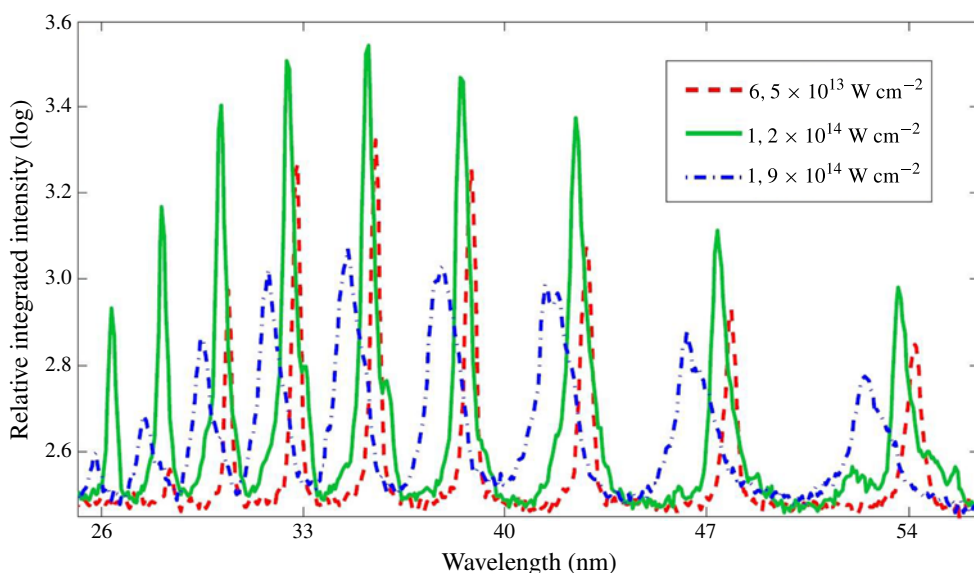


Figure 6. Increasing blue shift of high harmonics with increasing intensity for 12 bar Ar backing pressure.

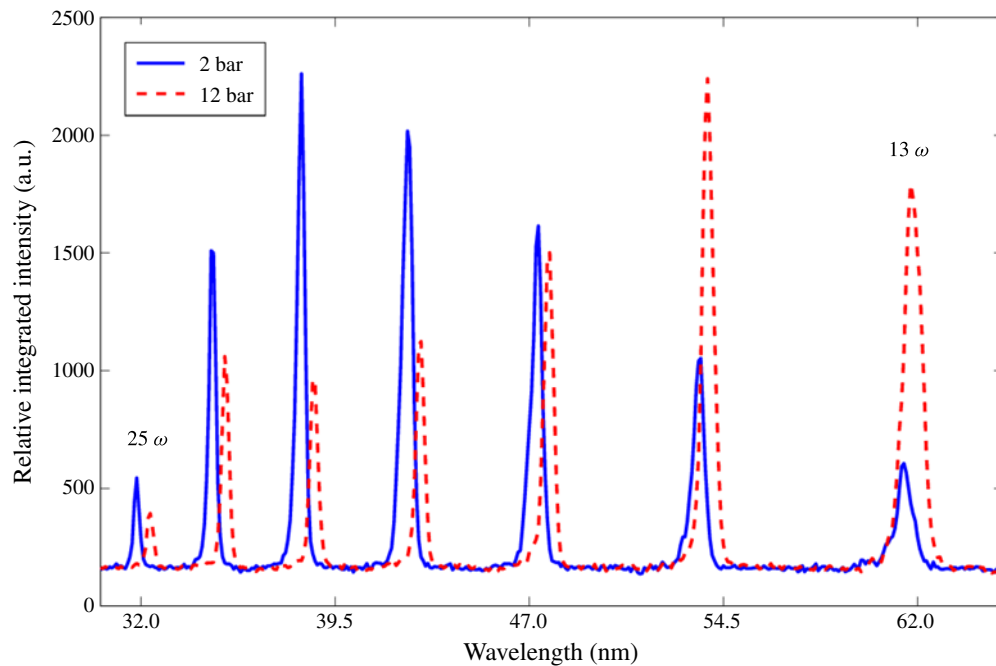


Figure 7. Harmonic spectra from Xe at $6.5 \times 10^{13} \text{ W cm}^{-2}$ intensity for 2 and 12 bar (dotted line) backing pressure.

shift of the harmonics can be observed which increases with increasing intensity. A special case of 12 bar backing pressure, i.e., high density of Ar, is illustrated here. It must be added that the spectral shift is dependent, in addition to the intensity, on the density of material and on the material as well, the results being different for different gases for the same backing pressure. Due to the strong density dependence, the blue shift is very sensitively dependent on the exact distance from the valve. Although the large spectral shift opens the possibility of tuning the harmonic wavelengths on the full observable spectral range in the VUV, application requires further studies with accurate measurement of the gas density.

An interesting phenomenon can be observed when at relatively low intensity we increase the backing pressure and thus the size of the clusters. Figure 7 shows the observed harmonic spectra from Xe in the case of $6.5 \times 10^{13} \text{ W cm}^{-2}$ intensity for low (2 bar) and high (12 bar) backing pressure. The spectral shift towards longer wavelengths is clearly visible.

In order to give a more quantitative insight we illustrate in Figure 8 the 21st harmonic in the case of xenon gas for the lowest intensity applied, i.e., $6.5 \times 10^{13} \text{ W cm}^{-2}$. We start with 2 bar backing pressure – when the clusters consist of a maximum of 1000 particles according to Figure 1 – as the one with zero spectral shift. On increasing the backing pressure a red shift, i.e., a spectral shift with the opposite signature to the one caused by the free electrons, can be observed. Although this type of spectral shift is always nearly an order of magnitude lower than the contribution

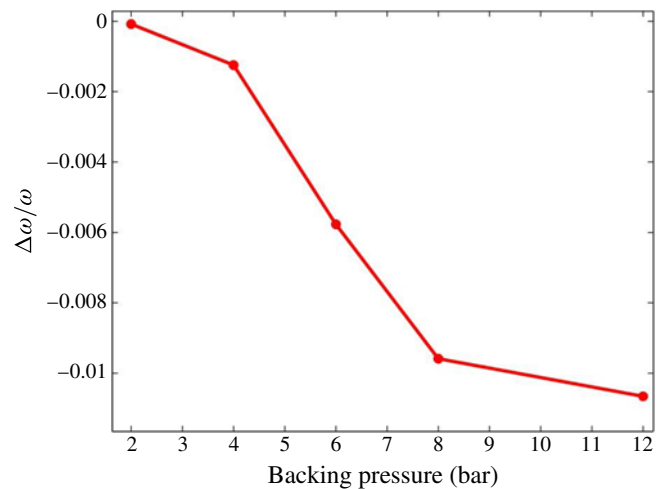


Figure 8. Red shift of the 21st harmonic for Xe at $6.5 \times 10^{13} \text{ W cm}^{-2}$ intensity with increasing pressure.

from free electrons it can be as high as $\Delta\omega/\omega \approx 10^{-2}$ for the highest applied pressure of 12 bar, in which case clusters with sizes of $\sim 10^5$ particles are expected. This contribution is expected to that caused by the nanoplasmas inside the clusters, as was suggested by Tisch^[18] and which we shall discuss below. It must be emphasized that as it is significantly lower than the blue shift caused by the free electrons it is only a relative red shift, often suppressed by the larger free-electron contribution, especially for higher intensities when the free electrons will dominate in the propagation effects.

4. Discussion

On the one hand, the experimental results confirm the earlier observations of intense HHG from cluster targets; on the other hand, the steep intensity increase of HHG with increasing pressure provides proof of the existence of clusters. The observation of a power law dependence, namely that the exponent is different from some earlier observations^[3], is probably only partially caused by the difference of the pulse duration of the applied lasers. As is evident from the spectral observations, the results are very sensitively dependent on the actual experimental parameters, especially the gas density and the cluster size.

Indeed, the most interesting result is the observed spectral structure of the generated harmonics. As is illustrated in Figure 6, the spectral shift caused by intensity variation is comparable with the distances between the subsequent harmonics. It should be borne in mind that by changing the gas and its pressure, this shift can be further increased, i.e., a quasi-continuously tunable coherent VUV and EUV light source can be generated. This may even serve as a seed pulse for an x-ray laser amplifier^[19].

The blue shift of the harmonics due to the free electrons, which increases both by increasing the pressure and by increasing the intensity, was explained by the phase matching condition, which for the laser and harmonics of order q can be given as

$$\Delta k = k_{q\omega} - qk_{\omega} = \Delta k_{disp} + \Delta k_{geom} + \Delta k_{electron}, \quad (1)$$

where $k_{q\omega}$ and k_{ω} are the wavevectors for the harmonics and the laser radiation, respectively. The subscript *disp* is the dephasing contribution from atomic dispersion, *geom* is the geometric contribution determined by the focusing geometry, and *electron* is the contribution from free electrons in the interaction range. Our main interest here is the free-electron contribution, which can be written as

$$\begin{aligned} \Delta k_{electron} &\approx \frac{6\pi}{\lambda_{\omega}} (n_{q\omega} - n_{\omega}) \\ &= \frac{6\pi}{\lambda_{\omega}} \left(\sqrt{1 - \frac{\omega_p^2}{q^2\omega^2}} - \sqrt{1 - \frac{\omega_p^2}{\omega^2}} \right) \geq 0. \end{aligned} \quad (2)$$

According to usual notation, ω_p is the plasma frequency. This term, as seen here, is always positive; thus, it gives a blue shift in frequency which can be approximated^[20] by

$$\Delta\omega_{electron} = \frac{\omega}{2n_e c} \frac{\partial \langle n_e \rangle}{\partial t} l, \quad (3)$$

in which the averaged density $\langle n_e \rangle$ along the pathlength l is given, which is a sort of self-phase modulation.

The effect of nanoplasmas inside the clusters on the dephasing was estimated by Tisch^[18], based on the simple

Drude model for the dielectric function, i.e.,

$$\varepsilon = 1 - \frac{\omega_p^2}{\omega(\omega + i\nu)}, \quad (4)$$

which, in general, uses the electron–ion collision frequency ν . The clusters are assumed to be dielectric spheres of radius r with a dipole moment of

$$p = \left(\frac{\varepsilon - 1}{\varepsilon + 2} \right) r^3 E_0, \quad (5)$$

for the field strength E_0 . Thus, the linear susceptibility can be estimated for the cluster density n_{cl} by

$$\chi_c = \frac{n_{cl} p}{E_0} = n_{cl} \left(\frac{\varepsilon - 1}{\varepsilon + 2} \right) r^3. \quad (6)$$

The refractive index can now be estimated for the collisionless case by

$$n(\omega) = \sqrt{1 + 4\pi\chi} \approx 1 + 2\pi\chi = 1 - \frac{2\pi n_e r^3 n_{cl}}{3n_{crit} - n_e}, \quad (7)$$

where n_e is the electron density inside the cluster and n_{cr} is the critical electron density. This means that $n(\omega) > 1$ for $n_e > 3n_{crit}$ and, on the other hand, $n(\omega) < 1$ for $n_e < 3n_{crit}$, where n_e is the electron density in the cluster. Consequently, we can estimate the dephasing as

$$\begin{aligned} \Delta k_{nanoplasma} &= \frac{6\pi}{\lambda_{\omega}} \left(1 - \frac{2\pi n_e r^3 n_{cl}}{3n_{crit} - n_e} \right) \\ &\quad - \frac{6\pi}{\lambda_{\omega}} \left(1 - \frac{2\pi n_e r^3 n_{cl}}{3n_{crit} - n_e} \right). \end{aligned} \quad (8)$$

The first term in Equation (8) is smaller than 1 due to the high frequency of the harmonics, and the second term is > 1 . Therefore, it has the opposite signature to Equation (2); consequently the nanoplasma can give a negative contribution with opposite sign to the free electrons in the interaction range. Thus, we can confirm that the spectral contribution of the nanoplasmas in the clusters can give a spectral shift of opposite signature to the free electrons; therefore, the observation of this red shift may also serve as evidence of cluster generation.

However, it must be noted that the above-mentioned blue and red shifts rarely appear separately in a clean form; they are strongly dependent on the parameters of the clusters and the lasers. Parametrization of the full range of observations can be carried out by using independent diagnostics of the cluster size. It must also be mentioned that in our estimations we used the simple analytical estimations of Tisch^[18]. Clearly, a full computer modelling of phase matching effects for different propagation geometries and different cluster sizes would be a great step forward.

5. Conclusion

We can conclude that the HHG in different gases gives a clear signature of the existence of clusters. Clusters can be used as a possible method to increase the conversion efficiency of HHG, but in this case the ionization threshold gives an upper limit, similarly to atomic gases.

Spectral investigation of high harmonics gives evidence of a possible tunable coherent radiation source in the whole VUV and EUV spectral range. The opposite signatures of the spectral shifts caused by the free electrons in the focal volume and the nanoplasmas inside the cluster can be applied as a further signature of cluster diagnostics, for which a comparison with the cluster size is under progress. As a further remark, it can be mentioned that a recent idea using dual-gas multijet arrays^[21] combined with cluster generation could become an even more efficient source of high harmonics.

Acknowledgements

This work, supported by the European Communities under the contract of the Association between EURATOM and the Hungarian Academy of Sciences, was carried out within the framework of the European Fusion Development Agreement. The views and opinions expressed herein do not necessarily reflect those of the European Commission. It was also supported by the Hungarian contract No. ELI 09-1-2010-0010 hELIOS-ELI, project 109257 of the Hungarian Scientific Research Fund and the COST MP1208 and MP1203 activities. P.R. was supported by a postdoctoral fellowship of the Hungarian Academy of Sciences.

References

1. K. J. Schafer, B. Yang, L. F. DiMauro, and K. C. Kulander, *Phys. Rev. Lett.* **70**, 1599 (1993).
2. P. Corkum, *Phys. Rev. Lett.* **71**, 1994 (1993).
3. T. D. Donnelly, T. Ditmire, K. Neumann, M. D. Perry, and R. W. Falcone, *Phys. Rev. Lett.* **76**, 2472 (1996).
4. C. Vozzi, M. Nisoli, J.-P. Caumes, G. Sansone, S. Stagira, S. De Silvestri, M. Vecchiocattivi, D. Bassi, M. Pascolini, L. Poletto, P. Villoresi, and G. Tondello, *Appl. Phys. Lett.* **86**, 111121 (2005).
5. Y. Wu, E. Cunningham, H. Zang, J. Li, M. Chini, X. Wang, Y. Wang, K. Zhao, and Z. Chang, *Appl. Phys. Lett.* **102**, 201104 (2013).
6. P. Rudawski, C. M. Heyl, F. Brizuela, J. Schwenke, A. Persson, E. Mansten, R. Rakowski, L. Rading, F. Campi, B. Kim, P. Johnsson, and A. L'Huillier, *Rev. Sci. Instrum.* **84**, 073103 (2013).
7. E. J. Takahashi, P. Lan, O. D. Mücke, Y. Nabekawa, and K. Midorikawa, *Nature Commun.* **4**, 3691 (2013).
8. H. Ruf, C. Handschin, R. Cireasa, N. Thiré, A. Ferré, S. Petit, D. Descamps, E. Mével, E. Constant, V. Blanchet, B. Fabre, and Y. Mairesse, *Phys. Rev. Lett.* **110**, 083902 (2013).
9. P. Moreno, L. Plaja, and L. Roso, *Europhys. Lett.* **28**, 629 (1994).
10. V. Vénier, R. Taieb, and A. Maquet, *Phys. Rev. A* **65**, 013202 (2001).
11. D. F. Zaretsky, Ph. Korneev, and W. Becker, *J. Phys. B* **43**, 105402 (2010).
12. R. Rakowski, A. Bartnik, H. Fiedorowicz, R. Jarocki, J. Kostecki, J. Mikolajczyk, A. Szczurek, M. Szczurek, I. B. Földes, and Zs. Tóth, *Nucl. Instrum. Methods A* **551**, 139 (2005).
13. O. F. Hagena, *Rev. Sci. Instrum.* **63**, 2374 (1992).
14. J. Peatross, J. L. Chaloupka, and D. D. Meyerhofer, *Opt. Lett.* **19**, 942 (1994).
15. F. Krausz and M. Ivanov, *Rev. Mod. Phys.* **81**, 163 (2009).
16. R. A. Ganeev, L. B. Elouga Bom, M. C. H. Wong, J.-P. Brichta, V. R. Bhardwaj, P. V. Redkin, and T. Ozaki, *Phys. Rev. A* **80**, 043808 (2009).
17. C. Altucci, R. Bruzzese, C. de Lisio, M. Nisoli, S. Stagira, S. de Silvestri, O. Svelto, A. Boscolo, P. Ceccherini, L. Poletto, G. Tondello, and P. Villoresi, *Phys. Rev. A* **61**, 021801(R) (1999).
18. J. W. G. Tisch, *Phys. Rev. A* **62**, 041802 (R) (2000).
19. Ph. Zeitoun, G. Faivre, S. Sebban, T. Mocek, A. Hallou, M. Fajardo, D. Aubert, Ph. Balcou, F. Burgy, D. Douillet, S. Kazamias, G. de Lacheze-Murel, T. Lefrou, S. le Pape, P. Mercere, H. Merdji, A. S. Morlens, J. P. Rousseau, and C. Valentin, *Nature* **431**, 426 (2004).
20. H. J. Shin, D. G. Lee, Y. H. Cha, J.-H. Kim, K. H. Hong, and C. H. Nam, *Phys. Rev. A* **63**, 053407 (2001).
21. A. Willner, F. Tavella, M. Yeung, T. Dzelzainis, C. Kamperidis, M. Bakarezos, D. Adams, M. Schulz, R. Riedel, M. C. Hoffmann, W. Hu, J. Rossbach, M. Drescher, N. A. Papadogiannis, M. Tatarakis, B. Dromey, and M. Zepf, *Phys. Rev. Lett.* **107**, 175002 (2011).